O3-type Na(Fe_1/3Mn_1/3Co_1/3)O_2 as a Cathode Material with High Rate and Good Charge-Discharge Cycle Performance for Sodium-Ion Batteries

Tsubota, Takayuki
Kobelco Research Institute

Kitajou, Ayuko
Organization for Research Initiatives, Yamaguchi University

Okada, Shigeto
Institute for Materials Chemistry and Engineering, Kyushu University

https://doi.org/10.5109/2547348

出版情報：Evergreen. 6 (4), pp.275-279, 2019-12. Transdisciplinary Research and Education Center for Green Technologies, Kyushu University
バージョン：

O3-type $Na(Fe_{1/3}Mn_{1/3}Co_{1/3})O_2$ as a Cathode Material with High Rate and Good Charge-Discharge Cycle Performance for Sodium-Ion Batteries

Takayuki Tsubota[1,3*], Ayuko Kitajou[2], Shigeto Okada[3]

[1]Kobelco Research Institute, Japan

[2]Organization for Research Initiatives, Yamaguchi University, Japan

[3]Institute of Materials Chemistry and Engineering, Kyushu University, Japan

*Author to whom correspondence should be addressed:

E-mail: tsubota.takayuki@kki.kobelco.com

(Received November 29, 2019; Revised December 8, 2019; accepted December 9, 2019).

Abstract: O3-$Na(Fe_{1/3}Mn_{1/3}Co_{1/3})O_2$ has been reported as a cathode material with a reversible capacity of 84mAh/g. This cathode active material shows excellent electrochemical performance with a high capacity retention of 95.0% after 100 cycles at 1C rate, and a discharge rate capability of 37mAh/g (47% of the initial capacity of 1C rate) at 50C rate. From the results of electrochemical impedance spectroscopy, an increase in reaction resistance was not confirmed between before and after the charge / discharge cycle test. TEM observation revealed that the crystal structure change on the surface of O3-$Na(Fe_{1/3}Mn_{1/3}Co_{1/3})O_2$ after the charge / discharge cycle test was slight, and the change in the crystal structure was small compared with that of the lithium ion battery, so O3-$Na(Fe_{1/3}Mn_{1/3}Co_{1/3})O_2$ has high crystal structure stability.

Keywords: sodium ion battery, cathode materials, electrochemical impedance spectroscopy

1. Introduction

Sodium ion batteries are regarded as a promising next-generation energy storage device to replace lithium ion batteries (LIB) due to their low cost. However, sodium ion batteries have the problem of low cycle life performance. There is a growing expectation that sodium-ion batteries, which run on widely abundant sodium, will be employed as low-cost secondary batteries[1]; therefore, $NaMeO_2$ compounds with a layered rock salt structure are being tested as cathode materials[2-7].

In addition, it is known that $LiFeO_2$ is electrochemically inactive—whereas $NaFeO_2$ is electrochemically active—when the Fe^{3+}/Fe^{4+} redox couple is used.[8] Many candidate O3-Type $NaMO_2$ cathodes for Na ion batteries have been reported, including $NaFe_{1/2}Co_{1/2}O_2$,[9] $NaFe_yNi_{1-y}O_2$,[10,11] $NaNi_{1/3}Co_{1/3}Fe_{1/3}O_2$,[12] $NaNi_{1/3}Mn_{1/3}Fe_{1/3}O_2$,[13] and $NaNi_{1/3}Mn_{1/3}Co_{1/3}O_2$.[14]

P2-Type $NaMO_2$ cathodes for Na ion batteries have also been reported: $NaxCoO_2$,[15-17] $Na_xMn_yCo_{1-y}O_2$,[18-21] $Na_{2/3}Fe_{1/2}Mn_{1/2}O_2$,[22] $NaxMn_yFe_{1-y}O_2$,[23-27] and $Na_{2/3}Mn_{1/3}Fe_{1/3}Co_{1/3}O_2$.[28]

Hence, Li-ion batteries with cathode materials (e.g., $Li(Ni_{1/3}Mn_{1/3}Co_{1/3})O_2$) that use transition metals such as Ni, Mn, and Co are used as electric-vehicle batteries; however, Na-ion batteries are electrochemically active even if these transition metals are replaced with Fe, as in the cases of $Na(Ni_{1/3}Mn_{1/3}Co_{1/3})O_2$ and $Na(Ni_{1/3}Mn_{1/3}Fe_{1/3})O_2$.

In this study, in order to clarify the cycle deterioration mechanism of $Na(Fe_{1/3}Mn_{1/3}Co_{1/3})O_2$, we assembled a test cell with hard carbon as the counter electrode and investigated the charge-discharge cycle characteristics. The cycle degradation mechanism was investigated using the nano-scale crystal structure of $Na(Fe_{1/3}Mn_{1/3}Co_{1/3})O_2$ before and after the cycle test, and the internal resistance was analyzed by electrochemical impedance spectroscopy.

2. Experimental

$(Fe_{1/3}Mn_{1/}3Co_{1/3})(OH)_2$ was synthesized using the coprecipitation method. A solution of $(Fe_{1/3}Mn_{1/3}Co_{1/3})(OH)_2$ in which each transition metal had a concentration of 0.5 M was prepared by dissolving $FeSO_4 \cdot 7H_2O$, $MnSO_4 \cdot 5H_2O$, and $CoSO_4 \cdot 7H_2O$ in ion-exchange water, at a stoichiometric ratio of 1:1:1. This was dripped along with a 3 M NaOH solution into a 0.2 M NaOH solution to prepare a hydroxide. After mixing this hydroxide with Na_2CO_3 in a ball mill, the precursor was baked at 900°C to obtain $Na(Fe_{1/3}Mn_{1/3}Co_{1/3})O_2$.

The cathode was prepared with an 85:10:5 wt% ratio of the synthesized active material, a conductive assistant, and a PVDF binder. To evaluate its electrochemical properties, a full-cells were assembled under an argon atmosphere, with the dew point adjusted to under -70°C, and the Hard carbon electrodes facing each other with a separator in the middle, to which an electrolyte (1 M $NaPF_6$/EC:DEC = 1:1 vol.%) was added. As a conditioning cycle, 3 cycles of charge and discharge were performed at 0.2C rate.

3. Results and Discussion

The typical discharge curves of the O3-$Na(Fe_{1/3}Mn_{1/3}Co_{1/3})O_2$ cathode at different current densities are shown in Fig. 1. The rate capability cycling performances of constant current cycled in the voltage range of 1.0 to 4.0 V are shown in Fig. 2. Even at 50C rate, the discharge capacity was 36.3 mAh/g, 47% of the initial capacity of the 1C rate, and good discharge rate characteristics were obtained.

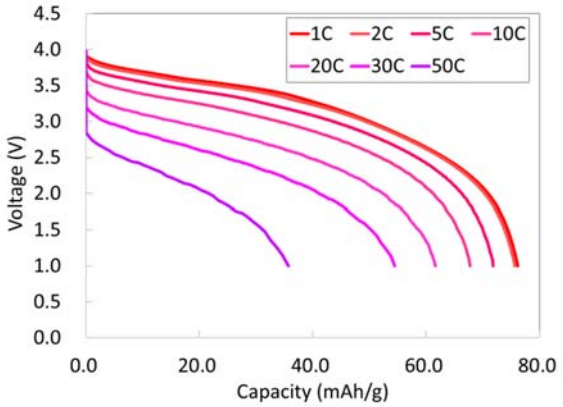

Fig. 1: Discharge curves at various current rates.

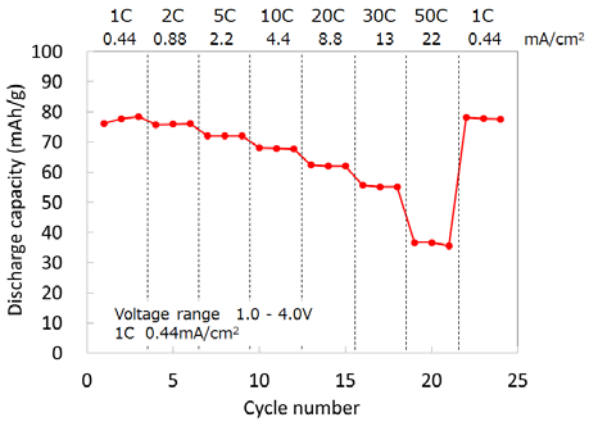

Fig. 2: Rate capacity plot showing cycling performance at various rates.

Figure 3 shows discharge curves in the 100 cycles at a current rate of 1C (0.44 mA/cm^2). Figure 4 shows the cycling performance and capacity retention at a current rate of 1C. The cycle performance retains a discharge capacity of 63.9 mAh/g after 100 cycles, 95.0% of the initial specific capacity, 100 % of the charge/discharge efficiency.

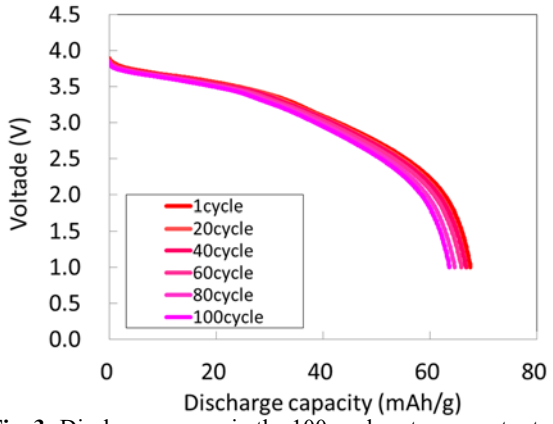

Fig. 3: Discharge curves in the 100 cycles at a current rate of 1C (0.44 mA/cm^2).

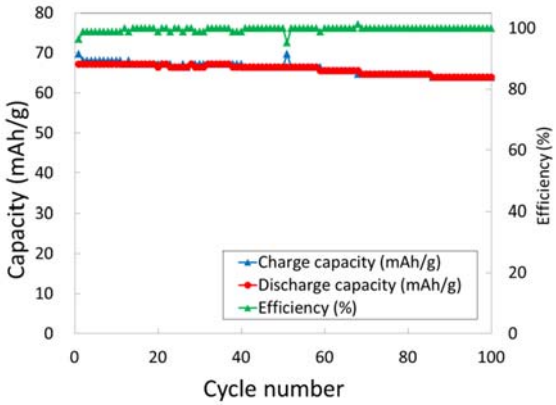

Fig. 4: Cycling performance and capacity retention at a current rate of 1C (0.44mA/cm^2).

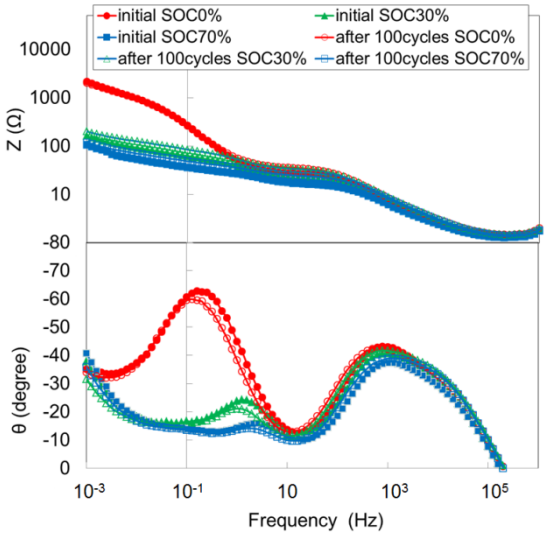

Fig. 5: Electrochemical impedance spectra of half cells at different charge states.

In order to investigate the reaction resistance of the O3-$Na(Fe_{1/3}Mn_{1/3}Co_{1/3})O_2$ cathode, a half cell combining the cathode taken out from the full cell and Na metal was reassembled, and electrochemical impedance spectroscopy (EIS) measurements were made.

The EIS measurements for the half cells cathode vs Na were collected in the potentiostatic mode with 10 mV amplitude about open-circuit voltage. Figure 5 shows EIS spectra for half cells at SOC (State of charge) 30%, 50%, and 70%. There was no significant increase in reaction resistance between before and after the cycle test.

To reveal the surface crystal structure of O3-$Na(Fe_{1/3}Mn_{1/3}Co_{1/3})O_2$, spherical aberration-corrected scanning transmission electron microscopy (Cs-STEM) was used. Figure 6(a) and 6(b) show the STEM-HAADF images of the initial image and the image after 100 cycles, respectively. Initially, a cubic phase was confirmed at 2 nm of the surface layer, and after the 100 cycles, a spinel phase of 5 nm was confirmed under the cubic crystal at 2 nm of the surface layer. The spinel phase and cubic phase is a deteriorated phase. The spinel phase and cubic phase inhibit the insertion and desorption of Na ions and increase the reaction resistance.

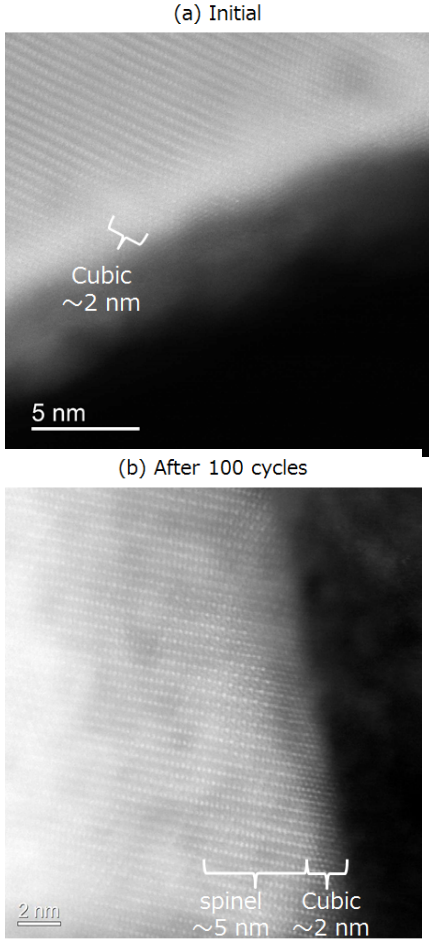

Fig. 6: STEM HAADF images of O3-$Na(Fe_{1/3}Mn_{1/3}Co_{1/3})O_2$ cathode materials initial state (a) and after 100 cycles (b).

Figure 7 shows the electron energy-loss spectroscopy (EELS) measurement points of the surface of O3-$Na(Fe_{1/3}Mn_{1/3}Co_{1/3})O_2$. Figures 8 and 9 show EELS spectra from the surface of $Na(Fe_{1/3}Mn_{1/3}Co_{1/3})O_2$ cathode materials of Mn-L, Fe-L, and Co-L edges initially and after 100 cycles, respectively. In the discharge state, the transition metals exist as high-spin Fe^{3+}, high-spin Mn^{4+}, and low spin Co^{3+}. On the surface layer, a shift to the low energy side of about 3 eV was confirmed in the spectrum of Mn. Therefore, Mn^{2+} exists on the surface layer. Similarly, a shift to the low energy side of about 1.5 eV was confirmed in the Co spectrum on the surface layer. Therefore, Co^{2+} exists in the surface layer. On the other hand, the shift to the low energy side was not confirmed in the spectrum of Fe. Therefore, Mn and Co are involved in the crystal structural change to the spinel phase and cubic phase on the surface layer, and Fe is not involved. It was found that the crystal structure change on the surface of O3-$Na(Fe_{1/3}Mn_{1/3}Co_{1/3})O_2$ after the charge/discharge cycles was slight, and the change in the crystal structure was small compared with that of the lithium ion batteries[29], so O3-$Na(Fe_{1/3}Mn_{1/3}Co_{1/3})O_2$ crystal structure has high stability.

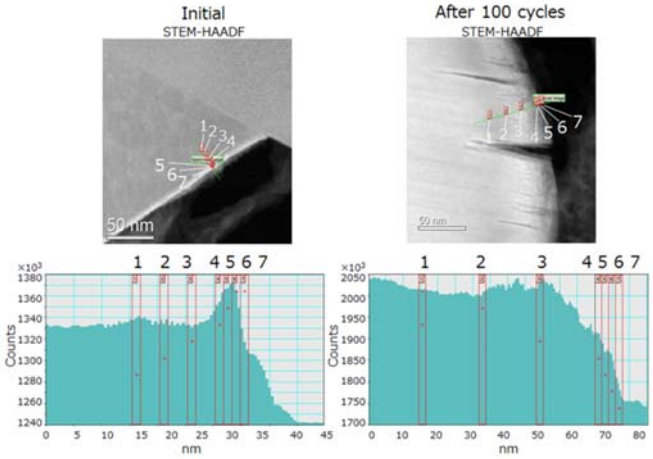

Fig. 7: EELS line profile points of initial state and after 100 cycles.

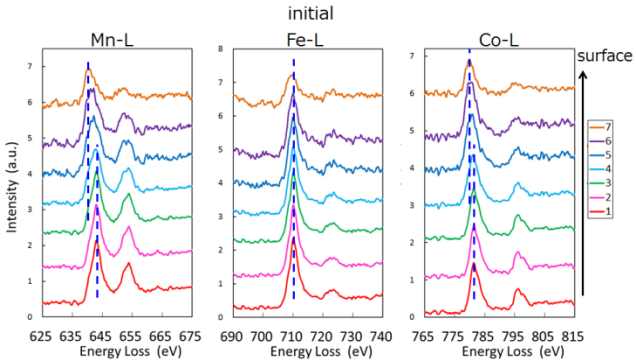

Fig. 8: EELS spectra from the surface of $Na(Fe_{1/3}Mn_{1/3}Co_{1/3})O_2$ showing the presence of Mn–L, Fe–L, and Co–L edges of initial state.

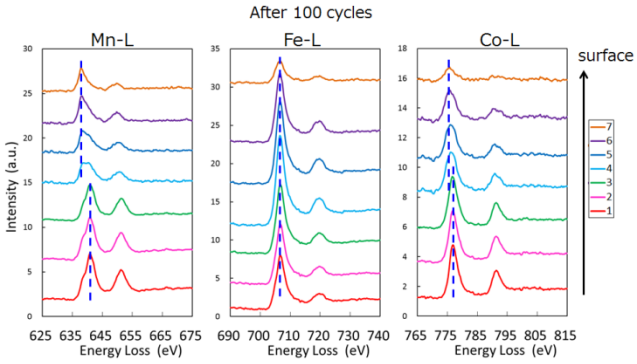

Fig. 9: EELS spectra from the surface of $Na(Fe_{1/3}Mn_{1/3}Co_{1/3})O_2$ showing the presence of Mn–L, Fe–L, and Co–L edges of after 100 cycles.

Since Fe element is not used in the layered rock salt structure cathode electrode of lithium ion batteries, the stability of Fe in the cathode electrode for sodium ion batteries was verified by first-principles calculations. The activation energy of the cation mixture was calculated by the first principle calculation. Figure 10 shows the calculated model of the layered rock salt structure of $Na(Fe_{1/3}Mn_{1/3}Co_{1/3})O_2$ in the charged state. Figure 11 shows the models used to evaluate the activation energies for transition metals from metal site to Na vacant site. Figure 12 shows the activation energies for transition metals from metal site to Na vacant site. The reaction path energies differ for each atom. Mn passed through the center of the octahedron, and Fe and Co passed through the midpoint of the oxygen atom. The activation energy of Mn was the lowest, which was in good agreement with the bonding state change in TEM-EELS. Figure 13 shows differences in electronegativity (Pauling) between transition metals and oxygen. Mn-O has a weak covalent bond and a small interaction.

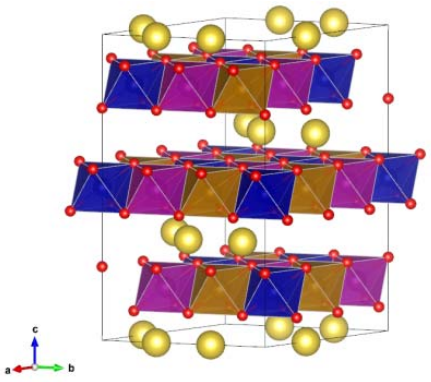

Fig. 10: The calculated model of the layered rock salt structure of $Na(Fe_{1/3}Mn_{1/3}Co_{1/3})O_2$ in the charged state.

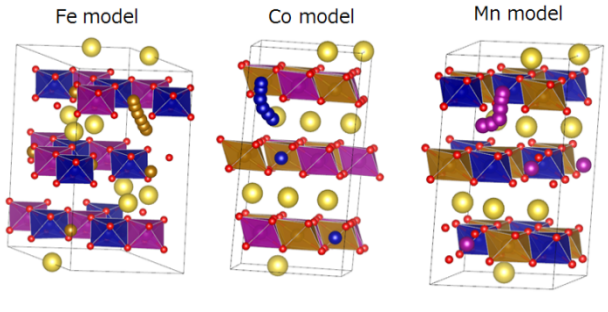

Fig. 11: Models for evaluating the activation energies of transition metals from metal site to Na vacant site.

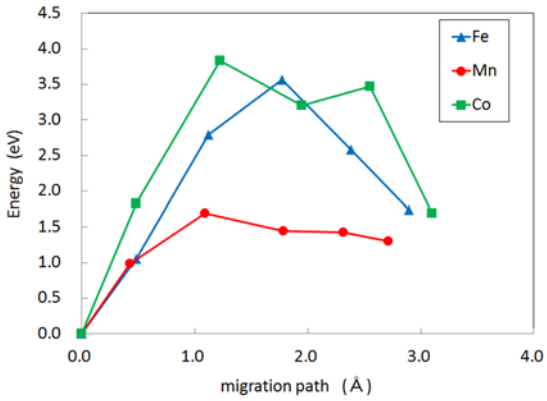

Fig. 12: The activation energies for transition metals from metal site to Na vacant site.

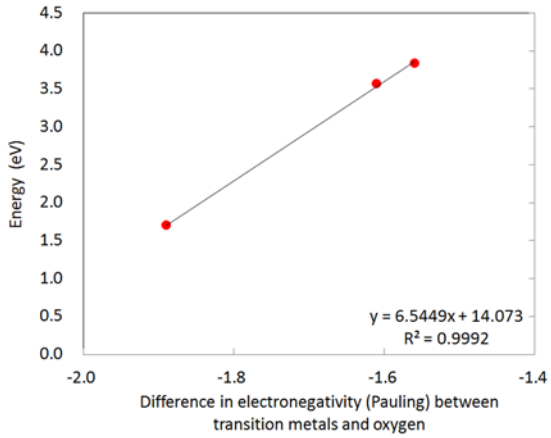

Fig. 13: Difference in electronegativity (Pauling) between transition metals and oxygen.

4. Conclusions

In summary, we have successfully synthesized a new O3-type layered rock salt structure of $Na(Fe_{1/3}Mn_{1/3}Co_{1/3})O_2$ for sodium ion batteries. This cathode active material shows excellent electrochemical performance with high capacity retention of 95.0% after 100 cycles at 1C rate, and a discharge rate capability of 37 mAh/g (47% of the initial capacity at 1C rate) at 50C rate. It was found that the crystal structure change on the

surface of O3-Na($Fe_{1/3}Mn_{1/3}Co_{1/3}$)O_2 after the charge/discharge cycle test was slight, and the change in the crystal structure was small compared with that of the lithium ion battery, so O3-Na($Fe_{1/3}Mn_{1/3}Co_{1/3}$)O_2 has high crystal structure stability.

References

1) K. Chihara, M. Ito, A. Kitajou, and S. Okada, *Evergreen*, **4**(1), 1 (2017).
2) S.-W. Kim, D.-H. Seo, X. Ma, G. Ceder, and K. Kang, *Adv. Energy Mater.*, **2** ,710 (2012).
3) S. Mariyappan, Q. Wand, and J.M. Tarascon, *J. Electrochem. Soc.*, **165**(16), A3714 (2018).
4) M. Slater, D. Kim, E. Lee, and C. S. Johnson, *Adv.Funct, Mater.*, **23**(26),3255 (2012).
5) S. Engelke, *storage4*, **1**(1),1 (2013).
6) H. Pan, Y.-S. Hu, and L. Chan, *Energy Environ. Sci.*, **6**,2238 (2013).
7) C. Nithya, S. Gopukumar, *Energy and Environment 4*, 253 (2015)
8) J. Zhao, L. Zhao, N. Dimov, S. Okada, T. Nishida, *J. Electrochem. Soc.*, **160**(5), A3077 (2013).
9) H.Yoshida, N.Yabuuchi, and S. Komaba, *Electrochem. Commun.*, **34**, 60 (2013).
10) S. Okada, Y. Takahashi, T. Kiyabu, T.Doi, J.Yamaki, and T.Nishida, *224th ECS meeting* (2016) Abstract #201.
11) X.Wang, G. Liu, T. Iwao, M. Okubo, and A. Yamaba, *J.Phys.Chem.C* , **118**, 2970 (2014).
12) P. Vassilaras, A. *J. Toumar, and G. Ceder, Electrochem. Commun.*, **38**, 79 (2014).
13) D. Kim, E. Lee, M. Slater, W. Lu, S. Rood, and C. S. Johnson, *Electrochem. Commun*., **18**, 66 (2012).
14) M. Sathiya, K. Hemalatha, K. Ramesha, J.-M. Tarascon, A.S. Prakash, *Chem. Mater.*, **24**, 1846 (2012).
15) R. Berthelot, D. Cariler, and C. Delmas. *Nature Mat.*, **10**, 74 (2011).
16) M. D'Arienzo, R. Ruffo, R.Scotti, F. Morazzomi, C.M. Mari, and S. Polizzi. *Phys. Chem. Chem. Phys.*, **14**, 5945 (2013).
17) J. J. Ding, Y. N. Zhou, Q. Sun, X. Q. Yu, X. Q. Yang, and Z. W. Fu, *Electrochimica Acta,* **87**, 388(2013).
18) J. M. Paulsen and J. R. Dahn, *Solied state Ionics.* ,**126**,3 (1999).
19) D. Carlier, J. H. Cheng, R. Berthelot, M. Guigard, M. Yoncheva, R. Stoyanova, B. J. Hwang, and C. Delmas, *Dalton Trans.*, **40**, 9306(2011).
20) X. Yang, M. Tamaru, M. Okubo, and A. Yamada, *J. Phys. Chem. C.*, **117**, 15545 (2013).
21) J. Cheng, C. Pan, J. Lee, J. Chen, M. Guignard, C. Delmas, D. Carlier, and B. Hwang, *Chem. Mater.*, **26**, 1219 (2014).
22) N. Yabuuchi, M. Kajiyama, J. Iwatate, H. Nishikawa, S. Hitomi, R. Okumura, R. Usui, Y. Yamada, and S. Komaba, *Nature Matt.*, **11**, 512 (2012).
23) N. Yabuuchi, J. Iwatate, M. kajiyama, Y. Yamamoto, S.Hitomi, R. Okumura, and S. Komaba, *220th ECS Meeting* (2011), Abstract #649.
24) J.S. Thorne, R. A. Dunlap, and M. N. Obrovac, *J. Electrochem. Soc.*, **160**, A361 (2013).
25) M. Sendova-Vassileva, R. Stoyanova, D. Carlier, M. Yoncheva, E. Zhecheva, and C. Delmas, *Adv. Sci. Tech.*, **74**, 60 (2010).
26) B.M. de Boisse, D. Carlier, M. Guignard, and C. Delmas, *J. Electrochem. Soc.*,**160**, A569 (2013)
27) J. Zhao, J. Xu, D. H. Lee, Y. S. Meng, and S. Okada, *224th ECS Meeting*(2013), Abstract #553.
28) J. S. Thorne, R. A. Dunlap, and M. N. Obrovac, *J. Electrochem. Soc.*, **161**(14), A2232 (2014).
29) T. Segi, R. Shu, T. Tsubota, and T. Yamaue, *JPS Conf. Proc.* **5**, 011014 (2015).